Low-Atmosphere Drifting Balloons: Platforms for Environment Monitoring and Forecast Improvement

A. Doerenbecher, P Basdevant, P. Drobinski, P. Durand, F Fesquet, F. Bernard, P. Cocquerez, N. Verdier, A. Vargas

LOW-ATMOSPHERE DRIFTING BALLOONS

Platforms for Environment Monitoring and Forecast Improvement

Low-atmosphere constant-volume balloons offer unique observing capabilities, such as Lagrangian sampling of air masses and data collection for weather prediction.

by A. Doerenbecher, C. Basdevant, P. Drobinski, P. Durand, C. Fesquet, F. Bernard, P. Cocquerez, N. Verdier, and A. Vargas

Balloon B21 (HyMeX SOP1) raising just after launch, on 14 Oct 2012 0614 UTC, Minorca (Spain).

CNES, the French Space Agency, has much experience with a variety of atmospheric balloons. These balloons generally serve as vehicles to carry potentially heavy scientific payloads from the planetary boundary layer (PBL) to the stratosphere. The reader can refer to the appendix for the meaning of acronyms.

We describe here long-range tropospheric balloons and more precisely constant-level superpressure (constant volume) balloons. The scope is to highlight the scientific interest of these PBL balloons including typical or novel scientific missions and to show examples of field campaigns that have taken place in the last 20 years.

A long-range balloon describes a balloon that does not rely on ground-based radio telecommunications for flight control but on satellite links, which allow global telecommunication coverage. CNES initiated the development of long-duration PBL balloons in 1972. The first flights took place in the Indian Ocean in 1975 (Cadet et al. 1981).

The illustration of the scientific capabilities of PBL balloons relies on several field campaigns, including ▶

Table 1. List of the field campaigns that involved BLPBs of CNES.				
Campaign	**Period**	**Area**	**Purpose and reference**	**Link**
INDOEX	Jan–Mar 1999	IO	Monitoring the low-level flow above Indian Ocean to study pollutant drift offshore India (Ethé et al. 2002)	http://www-indoex.ucsd.edu/
AMMA	Jun–Jul 2006	WA	Monitoring of low-level flow variability in relation with the onset of West African monsoon (Redelsperger et al. 2006)	http://amma-international.org/
VASCO	Jan–Mar 2007	IO	Monitoring of the low-level flow above Indian Ocean to study convection variability in relation with MJO (Duvel et al. 2009)	www.lmd.ens.fr/vasco/Home.html
TRAQA (ChArMEx)	Jun–Jul 2012	NWMed	Tracking of pollutant plumes above Mediterranean offshore France (Renard et al. 2015)	http://charmex.lsce.ipsl.fr
HyMeX (SOP1)	Sep–Nov 2012	NWMed	Moisture uptake and advection above the Mediterranean in relation with HPEs (Ducrocq et al. 2014)	www.hymex.org/
HyMeX (SOP2)	Jan–Mar 2013	NWMed	Monitoring of dry and cold winds that trigger oceanic convection in the NWMed3 (Estournel et al. 2015, manuscript submitted to *Oceanography*; Drobinski et al. 2014)	www.hymex.org/
ChArMEx (ADRIMED)	Jun–Jul 2013	NWMed	The aerosol direct radiative impact on the regional climate in the Mediterranean study of dust plumes (Renard et al. 2015)	http://charmex.lsce.ipsl.fr
ChArMEx (SAF-MED)	Jul–Aug 2013	NWMed	The secondary aerosol formation in the Mediterranean study focuses on organic aerosols and ozone life cycle (Gheusi et al. 2015)	http://charmex.lsce.ipsl.fr

INDOEX and VASCO in the Indian Ocean, AMMA in Africa, and TRAQA, HyMeX, and ChArMEx in the Mediterranean. Table 1 provides essential details such as the full name, date, location, purpose, a reference, and web links. Every campaign but AMMA took place above oceans, either the Mediterranean or the Indian Ocean. AMMA balloons were deployed above northwestern Africa during the summer of 2006.

Despite the fact that we focus on campaigns that, balloonwise, employed the strict use of CNES PBL balloons, other similar experiments carried out by other balloon agencies cannot be overlooked. In this respect, the United States, especially NOAA, has considerable experience with balloons. Thus, the paper by Businger et al. (2006) reviews numerous technical and scientific innovations that helped to advance the state-of-the-art lower-atmosphere drifting balloons.

The characteristics of the CNES PBL balloons are presented in the first part of this paper. Various scientific missions and data usages are then presented to illustrate the capabilities of the CNES low-level constant-volume balloons. At this stage, the in-flight behavior of the balloons will be discussed.

The last part of this paper discusses an original application of these balloons from an NWP perspective. Additional aspects of the setup and the proceedings of the HyMeX field campaign are

AFFILIATIONS: Doerenbecher—Centre National de Recherches Météorologiques, Météo-France, and CNRS, Toulouse, France; Basdevant, Drobinski, Fesquet, and Bernard—Laboratoire de Météorologie Dynamique/L'Institut Pierre-Simon Laplace, and Centre National de la Recherche Scientifique, and Ecole Polytechnique, Université Paris-Saclay, Palaiseau, France; Durand—Laboratoire d'Aérologie, University of Toulouse, and CNRS, Toulouse, France; Cocquerez, Verdier, and Vargas—Centre National d'Études Spatiales, Toulouse, France
CORRESPONDING AUTHOR: Dr. Alexis Doerenbecher, CNRM, Météo-France, 42 Avenue Gaspard Coriolis, 31057 Toulouse Cedex, France
E-mail: alex.doerenbecher@meteo.fr

The abstract for this article can be found in this issue, following the table of contents.
DOI:10.1175/BAMS-D-14-00182.1

A supplement to this article is available online (10.1175/BAMS-D-14-00182.2)

In final form 9 December 2015

Fig. 1. Simultaneous launch of two BLPBs during the winter SOP of HyMeX, on 14 Mar 2013 in Candillargues (France). Note the external scientific gondola at the top of the balloon and the shiny belt that is the rain deflector, as well as the nontransparency of the balloons as they are coated with a rain repellent. (Photo credit: CNES.)

provided in the supplemental material of this article (more information can be found online at http://dx.doi.org/10.1175/BAMS-D-14-00182.2).

LOW-ALTITUDE BALLOONS. CNES constant-volume balloons are also named BLPBs. Slightly differing versions of BLPBs exist, but the main features have remained the same for all of the 2012/13 field campaigns (Fig. 1). Flight characteristics are discussed at the end of this section.

The balloon's envelope. The spherical envelope of BLPBs (Fig. 2) is made of a semirigid, multilayer plastic that was chosen to withstand the internal pressure of the balloon and limit the leaks of the carrier gas. The typical diameter of the BLPB is 2.5 or 2.6 m. The latter is used to reach higher altitudes (from 2,000 to 3,300 m) and to carry potentially heavier weights. The carrier gas is a mixture of helium and ambient air that is tuned to achieve a predefined buoyancy corresponding to a flight level. The balloon's volume is quite constant as soon as the internal pressure of the carrier gas exceeds ambient air pressure. During HyMeX flights, a hydrophobic coating was applied to reduce the amount of liquid water (condensation, drizzle, or rain) on the surface of the balloon. The robustness of the envelopes allows almost weeks of flight.

This envelope is not meant for tunable buoyancy unlike the latest generations of NOAA smart balloons (Businger et al. 2006). The buoyancy of CNES BLPBs is set before launch thanks to precise tuning of the helium and air mixture that fills the balloon.

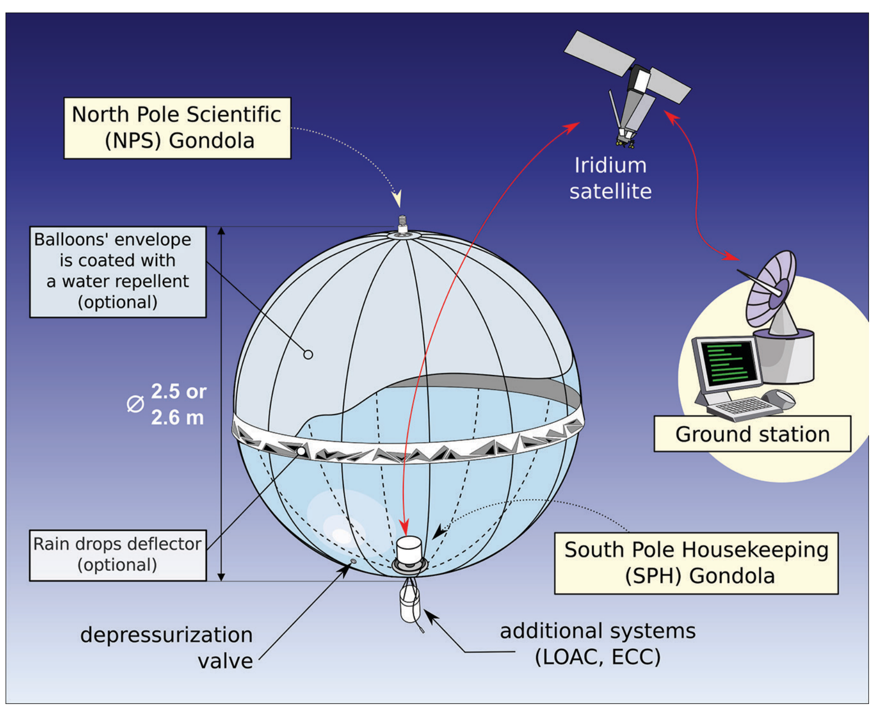

Fig. 2. Schematic diagram of the BLPBs used in TRAQA, HyMeX, and ChArMEx. The main technical features (e.g., gondolas) that intervene at some stage on the path of the data collection are detailed in Fig. 3.

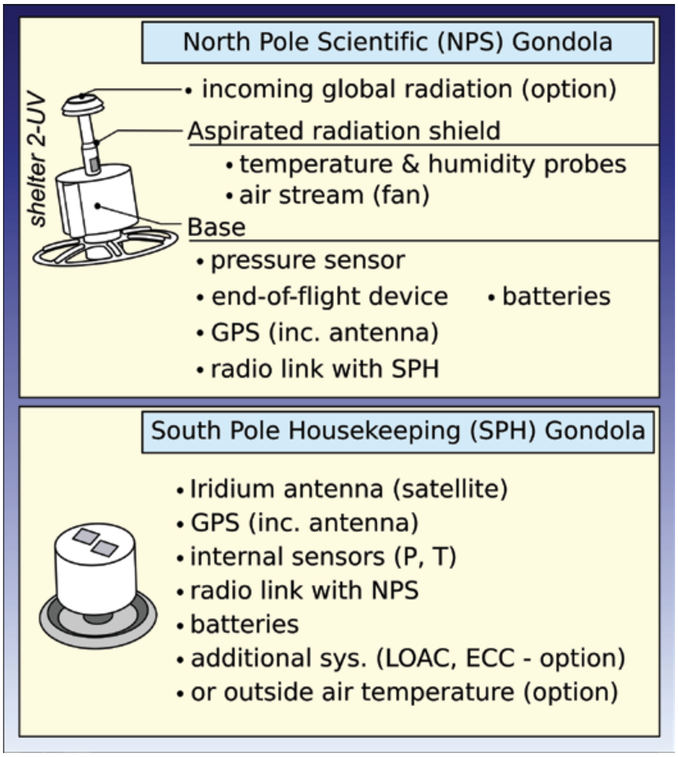

Fig. 3. (top) NPS gondola measuring atmospheric parameters and location. (bottom) SPH gondola containing housekeeping sensors, possibly additional sensors and the satellite communication (Iridium).

The payload. BLPBs have limited payload capacities and can only carry lightweight systems including all flight control (housekeeping) systems. This is also related to the fact that these balloons may fly in the most common air traffic domains. Either the balloon payload remains light [with respect to the air rules, annex 2, appendix 4, in ICAO (ICAO 2005) documentation, i.e., lighter than 4 kg] and no onboard air traffic management systems are required, or the payload is heavier and must be equipped with all the air traffic control facilities that imply the increase of the mass of onboard electronic systems as well as the size of the balloon. Consequently, the choice has been made to split the payload into two parts and to limit its size and mass to keep the BLPBs small. Figure 3 provides details on the contents and functions of the two parts of the BLPB payload. Figure 4 shows gondolas waiting for installation in the balloons.

The BLPBs integrate basic atmospheric sensors in their own structure in the form of a scientific gondola. During AMMA (Redelsperger et al. 2006; Lebel et al. 2010) and VASCO (Vialard et al. 2009; Duvel et al. 2009), the pressure, temperature, and humidity sensors were fixed at the end of three rods, pointing out of the balloon at its equator, where they were exposed to rain and dust. As rainy conditions were expected to be very common during HyMeX (Ducrocq et al. 2014), the integration of the sensors within a shelter was essential, so the latest version of the BLPBs includes a dedicated shelter at the top of the balloon (see Fig. 3). Table 2 summarizes the characteristics of the scientific payloads (gondolas) throughout the field campaigns (campaign information is available in Table 1).

The meteorological shelter is a part of the NPS gondola designed by the CNES. The temperature and humidity sensors are

Fig. 4. Gondolas used during SAF-MED (2013) before being mounted on the balloons. SPH gondolas are in the front row. The cover of the base of the NPS is in a lifted position, so the batteries are visible, and the aspired radiation shield that contains the temperature and humidity sensor is hidden. The global radiation sensor can be seen at the top of the NPS gondolas. (Photo credit: CNES.)

fitted inside the ventilated tubular part of the shelter. Several forms of the shelter itself have been tested and implemented in order to minimize its size and to mitigate radiative heating in sunlight or infrared cooling at night. The pressure sensor is located at the base of the NPS gondola (see Fig. 3). Table 3 shows the manufacturers' specifications for the three sensors inserted in the NPS gondola as well as the specifications for the positioning system for the 2012 and 2013 campaigns. Table 3 shows that the application range of the sensors is limited. However, these intervals are coherent with the scientific mission of the balloons in campaigns where the highest flight (ChArMEx ADRIMED) reaches the lower bound for the pressure, and the coldest flight (HyMeX SOP2) is close to 0°C, which is the lower boundary for the temperature application interval.

Two GPS receivers locate precisely the balloon in three directions (latitude, longitude, and altitude). The nominal GPS receiver is fitted in the NPH gondola, outside, at the top of the balloon (just below the NPS). The so-called SPH gondola includes the spare GPS receiver. The collection of the GPS data also allows horizontal wind estimates along the balloon trajectory.

The ChArMEx balloons had dedicated scientific payloads fitted below the lowest pole (bottom) of the balloon. This payload consisted of either ozone sensors or particle counters (Gheusi et al. 2015, manuscript submitted to *Atmos. Meas. Tech.*; Renard et al. 2015, 2016).

Telecommunications. The SPH gondola (see Fig. 3) controls the flight and receives or sends information. In the early days, telecommunications used a line-of-sight radio link (Bénech et al. 1987). The limited range of this communication system prevented long-distance flights, especially in proximity to the ground. To avoid this limitation, use of the Argos system was implemented for INDOEX (Ethé et al. 2002) and in 2012 was replaced by the Iridium constellation (see Table 2), which offers better global coverage.

In the latest version of BLPBs, the data are sampled twice every minute and stored on board. The meteorological data acquired by the external gondola are sent to the housekeeping gondola through a UHF link (see Fig. 2). Since telecommunication is an important part of the

Table 2. Summary of the balloons' characteristics: size, payload, and sensor for every campaign. SPS means the payload is fixed at the south pole (bottom) of the balloon, EQR means that the sensors are set at the equator of the balloon at the end of horizontal rods, and NPS means that the sensors are located at the north pole (top) of the balloon, in a dedicated shelter, where the number tells the generation of the shelter [first (1) or second (2)]. Sensors measure temperature *T*, pressure *P*, and relative humidity (*Hu*)

Campaign	Balloon no.	Launch site	Main gondola	Sensors (position)	Positioning system	Satellite link	Weight (kg)	Size (m)	Extra (SPS) payload	Extra (NPS) payload
INDOEX	17	Goa (India)	Internal	*T*, *P*, *Hu* (EQR)	GPS	Argos	~9	2.5	No	No
VASCO	10	Mahé (Seychelles)	Internal	*T*, *P*, *Hu* (EQR)	GPS	Argos	9	2.5	No	No
AMMA	15	Cotonou (Benin)	Internal	*T*, *P*, *Hu* (EQR)	GPS	Argos	9	2.5	No	No
TRAQA (ChArMEx)	5	Sausset (France)	Internal	*T*, *P*, *Hu* (NPS 1)	GPS	Iridium	9–9.5	2.5	No	No
HyMeX (SOP1)	19	Maò (Spain)	Internal	*T*, *P*, *Hu* (NPS 1)	GPS	Iridium	9–9.5	2.5	No	No
HyMeX (SOP2)	16	Candillargues (France)	Internal	*T*, *P*, *Hu* (NPS 1 + 2)	GPS	Iridium	9.5–10	2.5	No	No
ChArMEx (ADRIMED)	14	Maò (Spain)	Internal	*T*, *P*, *Hu* (NPS 2)	GPS	Iridium	8	2.5 or 2.6	LOAC or ECC	Solar flux
ChArMEx (SAF-MED)	12	Île du Levant (France)	Internal	*T*, *P*, *Hu* (NPS 2)	GPS	Iridium	8	2.5	LOAC or ECC	Solar flux

balloon's energy budget, it is necessary to reduce the communication rate for flights longer than 7 days in order to save energy. All scientific payloads (either the NPS or additional payload fixed below the balloon) rely on the communication facilities offered by the housekeeping systems to send scientific data to the ground.

(For further details, the reader can refer to the following web page: www.lmd.polytechnique.fr/BAMED/HISTOIRE/BP_Techno.php.)

Flight range and end of flight. Table 4 lists the duration of every flight operated during AMMA and VASCO 2007. The longest flight lasted for more than 1 month. However, most of the flights were shorter, especially in AMMA. The reader will find the INDOEX flight durations in Fig. 2 of Ethé et al. (2002). Figure 5 shows the typical distance, duration, and altitude of the BLPB flown in the Mediterranean. Four out of the five campaigns requested flights below 1,000 m. Larger circles more to the left indicate slower flights. The flight duration during both HyMeX SOPs was short (less than two days) as the balloons could only fly above the sea for safety reasons.

Under optimal conditions, the balloons are capable of long flights (more than one month in duration; see Table 4) limited only by the lifetime of the onboard batteries. Renewable energy devices have not yet been implemented by CNES. During the last Mediterranean campaigns, the flights were only one day long on average (Fig. 5). Energy consumption was not a problem, and telecommunication could be used at a high rate (every 20 min).

Flight termination can be triggered either by the balloon operator or by automated procedures. In the Mediterranean, the balloons were programmed with the authorized flight domain, and any drift outside this domain automatically initiated the deflation of the balloon. Deflation is triggered by melting a small piece of the envelope through the use of a hot wire. BLPBs are disposable systems and are not intended to be recovered at the end of their flight. In practice, energy consumption, safety issues, and the authorized flight domain control the duration of the BLPBs' flights, rather than the robustness of the envelope itself. Despite the fact that BLPBs are small balloons (see section titled "The payload"), CNES continuously informs air traffic control and authorities of the balloon status (3D position and flight termination).

SCIENTIFIC APPLICATION: LAGRANGIAN APPROACH. As a consequence of its constant volume, BLPBs float on constant-density (isopycnal) levels. The balloon drifts within an air parcel. In order for the balloon to drift in a Lagrangian manner, the air parcel should not be affected by any vertical winds. The Lagrangian property does not apply when the balloon is ascending from the ground to its equilibrium buoyancy level or when the balloon is deflated. All atmospheric perturbations that push the balloon out of its equilibrium disturb Lagrangian behavior. Convective uplifts or downdrafts, waves (e.g., in the lee of mountains or islands), or diabatic processes involving liquid or solid water that stick to the balloon skin and change its buoyancy are the most common causes for non-Lagrangian flight behavior.

A technical advance would be to implement double-envelope (air and helium) devices to allow for (limited) control of the altitude. For instance, the flight level of BLPBs depends on the buoyancy, which depends on the initial air–helium mixture. It is therefore impossible to change the flight level after the launch. Such a possibility would, however, be useful in the case of persistent change in the flying mass, when there are multiple scientific missions in

Table 3. Manufacturer specifications for the sensors in the NPS used in TRAQA, HyMeX, and ChArMEx. GPS was used to derive wind estimates. In ChArMEx the NPS included a global radiation sensor (not shown here).

	Parameter	Range	Precision	Resolution	Make/feature
Air	Temperature (°C)	0–50	±0.5	0.1	Rotronic/HC2-S
	Relative humidity (%)	0–100	±2.5	0.5	Rotronic/HC2-S
	Pressure (hPa)	700–1,100	±1.0	0.1	Measurement Specialties/MS5540C
Positioning	Longitude (°)	0–360	≤6.0 m (50%) ≤9.0 m (90%)	3.7 m	GNSS: Ublox/LEA-6H; and
	Latitude (°)	0–90	≤6.0 m (50%) ≤9.0 m (90%)	3.7 m	GNSS Patch Antenna: Spectrum Control, Inc./PA 23–1575–008S A
	Altitude (m)	0–4,096	≤11.0 m (50%) ≤18.0 m (90%)	1	

a single flight, or when one wants to avoid losing the balloon (e.g., hitting the ground).

Another important condition to guarantee Lagrangian behavior is the balloon itself not influencing the air parcel with which it travels. This last condition is important, especially in terms of temperature and relative humidity measurements. It is widely accepted that in situ observing systems are easily influenced by solar radiations (even radiosounding temperature data are corrected for radiative biases). Aspirated radiative shields help to reduce radiative temperature biases. Concerning semitransparent balloons, radiative influence is significant, and some convection can occur along the balloon skin. This convection may impact the quality of the temperature data, unless the sensors are ventilated to mitigate the effects of the convection. The five Mediterranean experiments in 2012/13 with similar instrumental configurations but very different flight conditions helped to estimate the biases introduced by the balloon.

Study of pollutants and dusts: ChArMEx. The first phase of ChArMEx (ADRIMED) studied the southerly transport of dust (e.g., Saharan dust) above the sea, with a focus on aerosol radiation measurements and modeling. There were 14 balloons deployed from Minorca (Balearic Islands) in conditions of generally moderate wind and clear sky. Flight levels ranged from 2,000 to more than 3,000 m MSL (Fig. 6, left). Two balloon sizes were used: 2.5 and 2.6 m for ceiling flight altitudes of approximately 2.5 and 3 km, respectively.

The second phase of ChArMEx (SAF-MED) tackled pollution issues, as did the TRAQA campaign (see section on "TRAQA campaign: An example of pollutant tracking") the year before. The 12 BLPBs were launched from the Île du Levant (military site on the French Riviera). Flight levels were between 600 and 1,000 m MSL (Fig. 6, right). Trajectorywise, it was a challenge to reach the

Table 4. List of the flight duration (days) for AMMA and VASCO.

Flight	Campaign	
	AMMA 2006	VASCO 2007
BP01	0.8	33.2
BP02	5.2	4.1
BP03	4.6	15.9
BP04	2.0	6.5
BP05	7.2	11.2
BP06	8.3	12.2
BP07	1.9	4.1
BP08	15.2	20.6
BP09	1.9	17.9
BP10	2.2	17.9
BP11	2.9	—
BP12	5.1	—
BP13	4.2	—
BP14	0.5	—
BP15	2.2	

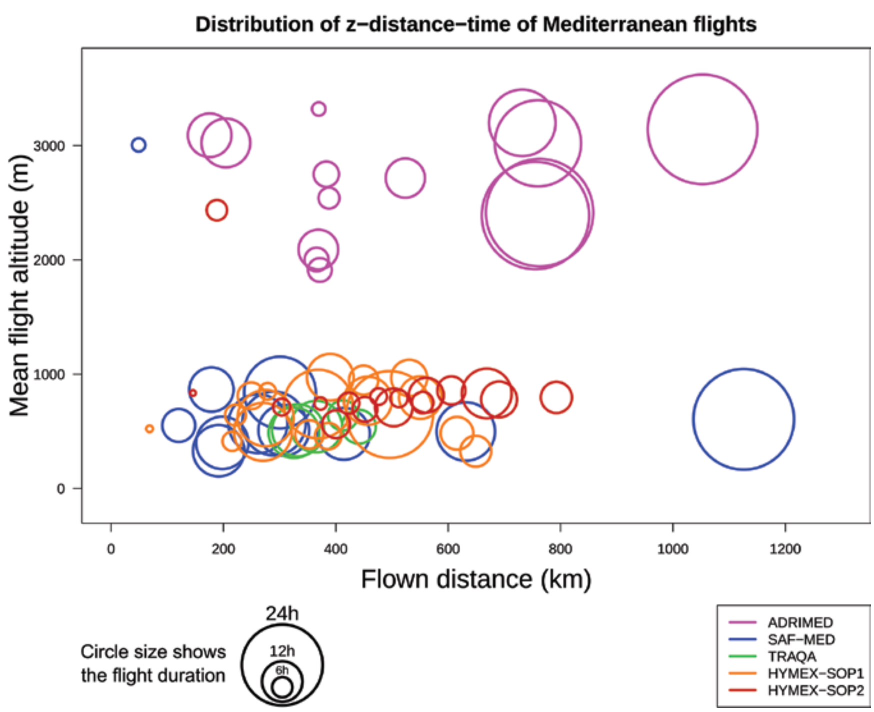

Fig. 5. Flight characteristics of the 2012/13 Mediterranean campaigns. Each circle refers to one flight. Colors indicate the campaign, and the diameter indicates the flight duration (scale in black below the graph). The position of the circles indicates the distance traveled and the mean flight level. Speedy balloons are shown as small circles on the right of the frame, while slow balloons are large circles on the left.

Sicily basin because the balloons had to pass between Corsica and Sardinia and the Strait of Sicily, where the flight domain was significantly narrower.

Thirteen BLPBs (10 in ADRIMED, 3 in SAF-MED) were equipped with an optical particle counter known as the LOAC, recently developed by the LPC2E. This instrument is able to measure the size distribution of aerosols in a range from a few tenths to some tens of micrometers as well as to infer the nature of the aerosol from the light observed at two scattering angles (Renard et al. 2016). The LOAC measurements revealed an unexpected persistence of coarse particles inside several desert dust plumes with diameters of between 15 μm and several tens of micrometers (Renard et al. 2015).

Thirteen BLPBs (4 in ADRIMED, 9 in SAF-MED) were fitted with an ECC ozonesonde (Gheusi et al. 2015, manuscript submitted to *Atmos. Meas. Tech.*). The ECC ozonesonde, which has previously been placed on drifting balloons (Bénech et al. 2008), has been modified so as to last longer, due to the intermittent data collection mode. The ChArMEx campaigns succeeded in capturing the first Lagrangian observation of ozone photo production in the free troposphere (Gheusi et al. 2015, manuscript submitted to *Atmos. Meas. Tech.*).

Individual flight data and graphs can be viewed online (see www.lmd.polytechnique.fr/BAMED/CHARMEX_BP_Flight_SOP1.php for ADRIMED and www.lmd.polytechnique.fr/BAMED/CHARMEX_BP_Flight_SOP2.php for SAF-MED).

TRAQA campaign: An example of pollutant tracking. In the TRAQA campaign, five BLPBs were deployed from Sausset-les-Pins (France) in two cases of weakening mistral (clear sky, moderate wind). The purpose was to study the time evolution (ageing) of pollutants within drifting air parcels offshore. The source of the pollutants was the Fos-Berre industrial area, in the vicinity of the launch site. The balloons were deployed as tracers to identify the air parcels as described in Businger et al. (1996) and to follow them as they left the continent and traveled above the Mediterranean Sea. The balloons collected pressure, temperature, and humidity as well as ozone data. The SAFIRE ATR42 research aircraft (www.safire.fr) flew several times during the BLPB flights to collect additional data (Gheusi et al. 2015, manuscript submitted to *Atmos. Meas. Tech.*). The aircraft used the balloons as targets with which to reach the air parcels to sample. Figure 7 shows the flight trajectories in the two cases studied in TRAQA.

ATR42 flights are shown as red and green lines with colored dots that indicate the aircraft position every minute when the flight level is lower than 800 m. The color shows the time of day and overlapping trajectories with similar colors signifying collocation. The mean flight level of the balloons was

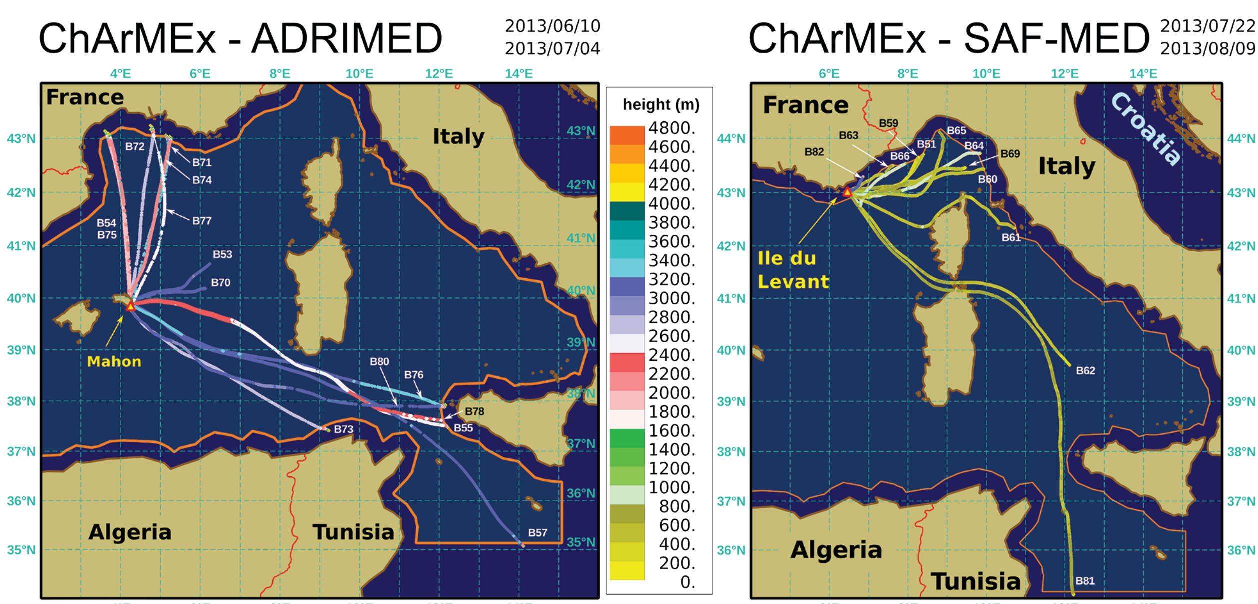

Fig. 6. Trajectories of the flights made during ChArMEx (left) SOP1 (14 flights) and (right) SOP2 (12 flights). The trajectory colors show the flight level (m; scale is on the right). The launch site is shown as a red triangle: San Luis airfield, close to Mahon on Minorca, in SOP1, and the Île du Levant, an island along the French Riviera, in SOP2. The orange line shows the limits of the flight domain where most of the flights end as a consequence of the automated end-of-flight procedure implemented in the BLPBs' computer.

500 m, except in the flight known as B10 (on 27 July 2012), which flew at about 600 m.

Monitoring of ambient flow for process studies: INDOEX and VASCO. The intensive field phase of the INDOEX (Lelieveld et al. 2001) took place from January to March 1999. INDOEX was a multiyear project focusing on the transport and evolution of anthropogenic and mineral pollutant (aerosols) emitted from the Indian subcontinent.

The 17 BLPBs were launched from Goa (southeastern India) in northeasterly wind flow (Ethé et al. 2002). Most of these balloons reached the Arabian Sea (and even ITCZ) in approximately 7 days, drifting at low levels (950–800 hPa). Temperature, pressure, humidity data, and position (including extra parameters with which to manage the balloon's flight) were collected every 30 min, but no aerosol data were collected. They served as Lagrangian tracers for pollutant plumes and observation of ambient flow to validate modeled atmospheric transport. The comparison with ECMWF analyses allowed an evaluation of the systematic temperature and wind biases (Ethé et al. 2002).

The VASCO-Cirene joint field experiments in January–February 2007 investigated the MJO-related SST and convection events along the Seychelles–Chagos thermocline ridge. VASCO consists of the balloonborne atmospheric campaign (Duvel et al. 2009) and Cirene is the oceanic part involving a research vessel (Vialard et al. 2009). VASCO used BLPBs and Aeroclippers, two types of balloons drifting in the boundary layer. The Aeroclipper is a streamlined balloon tethered to a drifting marine gondola and is not Lagrangian because of the surface drag. The Aeroclipper collects data at approximately 50 m above the sea surface. Measurements of pressure, temperature, humidity, and wind were collected by these balloons in order to validate the meteorological fields provided by ECMWF and were used to describe the large-scale environment for the Cirene cruise measurements (Vialard et al. 2009).

During VASCO, 10 BLPBs and 8 Aeroclippers were launched from Mahé (in the Seychelles). Two BLPBs flew up to 20,000 km and for up to one month (see Table 4). The balloons provided statistics on surface- and low-level atmospheric perturbations related to intraseasonal oscillations at the very large scale, on equatorial wave perturbations at the synoptic scale, and on convective systems at the mesoscale. Eventually, the balloons allowed the monitoring of the birth and evolution of two tropical cyclones, Dora and Gamède (Duvel et al. 2009).

OTHER SCIENTIFIC APPLICATIONS.

AMMA: Space–time variability in West Africa. During AMMA (Redelsperger et al. 2006), a wide range of instruments was deployed throughout West Africa. Among them, 15 BLPBs were launched from Cotonou (Benin) in the PBL between mid-June and mid-July

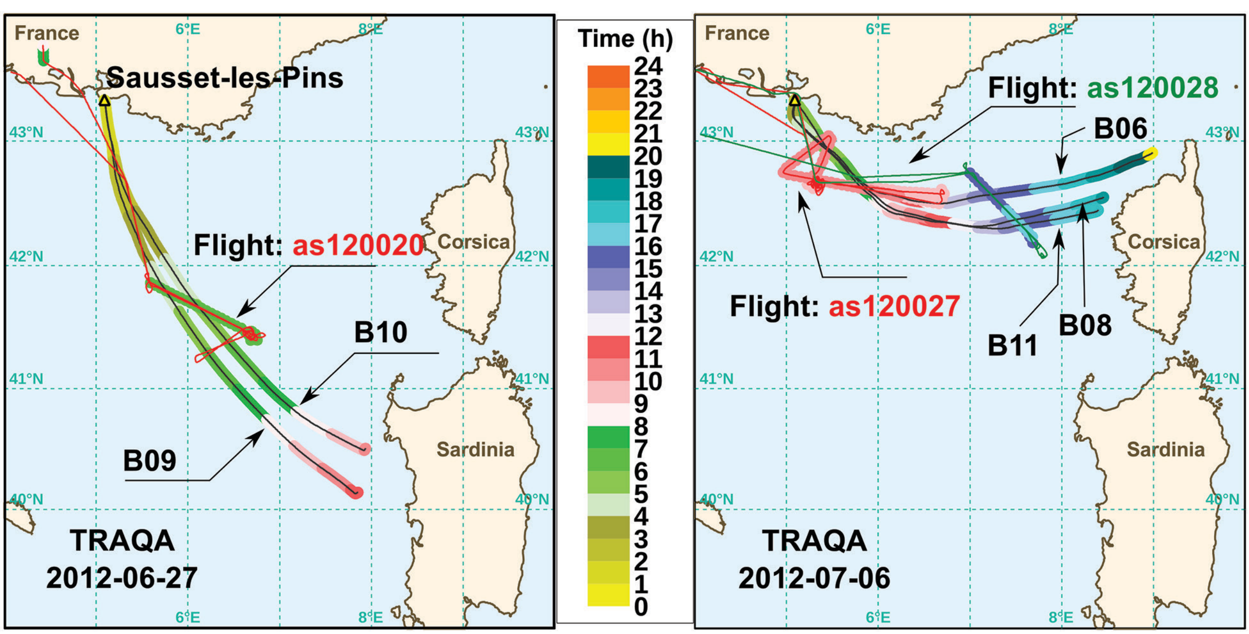

Fig. 7. Trajectories of the five BLPBs deployed during the TRAQA field campaign (Jun–Jul 2012) overlaid with flight tracks of the ATR42 aircraft. The atmospheric flow was quite slow (moderate or diminishing mistral situation) at about 500 m. The colors show the time in the day (h) and positions below 800 m for the ATR42.

2006, allowing Lagrangian measurements of wind, temperature, and humidity. Three BLPBs reached the ITD, separating the southwesterly monsoon flow from the northeasterly Harmattan. The data collected by the BLPBs were used to investigate the multiscale variability of the monsoon's circulation and in particular the diurnal cycle of West African monsoon dynamics. They were also used to validate meteorological analyses. Figure 8a displays the trajectory of BLPB 8, and Fig. 8b shows the time series of its flight altitude. The drop in balloon altitude on 1 July 2006 (circled in green) suggests that the balloon met a convective system over the eastern border of Benin (confirmed by Meteosat Second Generation satellite imagery). North of 11°N, the trajectory takes an eastward direction and resembles a cycloid due to the more pronounced diurnal cycle of the wind over the Sahel. After a few days, it reaches the Ouaddaï massif (eastern Chad) and its trajectory becomes irregular due to local mountain-induced circulations. Once it has reached the ITD, the variations of the trajectory may be due to the longitudinal variability of the location of the ITD, the diurnal variability of its location, and the mountain environment.

Data collected along the BLPB trajectories showed a very well marked, height-dependent diurnal cycle of the PBL wind, with different characteristics (e.g., limited latitudinal influence of the southwesterly nocturnal jet) as they move northward, in coherence with previous studies (Sultan et al. 2007). The statistical comparison between the BLPB and the 900-hPa ECMWF analyses wind speed is shown in Fig. 9, divided into four periods of the day. The mean flow is well described by the model, especially in the daytime (1200 and 1800 UTC), when the distribution of the model observation departure is quite narrow. The distributions are much broader during the night (0000 and 0600 UTC). This may be explained by the fact that the BLPB pressure level is not exactly that of the model. The intensity of the nocturnal jet is height dependent as it is confined in a layer 300 m thick, so an altitude discrepancy may induce a wind difference. Moreover, another model wind deficiency was brought out by the divergence of isopycnic trajectories computed with ECMWF analyses at three levels (approximately 1,000, 925, and 850 hPa) from the BLPB trajectories (not shown here). In particular, ECMWF trajectories are often more northward than

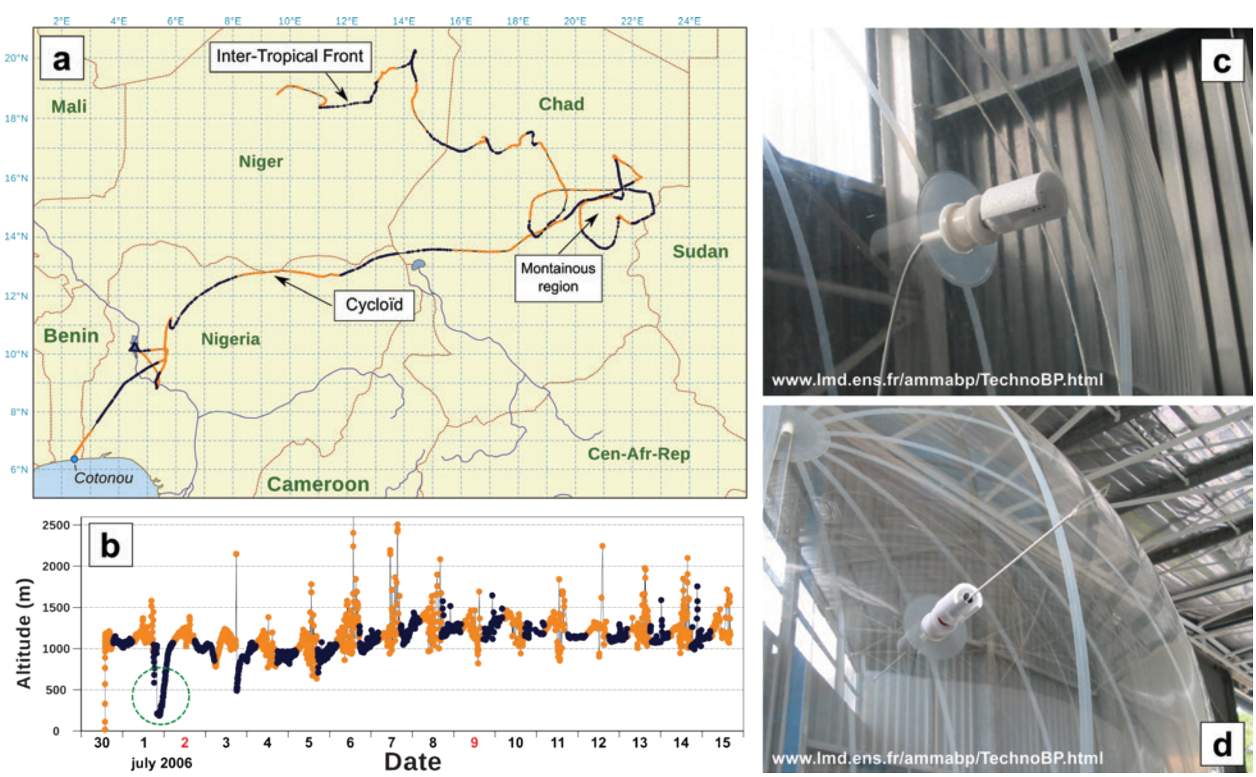

Fig. 8. (a) Map showing the trajectory of BLPB 8 during AMMA (2006) as a function of time (orange is daytime; black is nighttime). This is the longest flight recorded during AMMA (see Table 4). (b) Time series of BLPB 8 flight level (altitude shown in meters) depicting the high variability of the flights above land. The green circle shows the drop of flight altitude when encountering a convective system (see text). (c),(d) Pictures of the hygrometer and the thermometer on the AMMA BLPBs that are fitted on the equator of the balloon. (Photo credit: CNES.)

those of BLPBs, especially near the coastline and in the eastern part of the Sahel region.

Water vapor and dynamics: HyMeX SOP2. The second SOP of HyMeX (Estournel et al. 2015, manuscript submitted to *Oceanography*; Drobinski et al. 2014) was dedicated to the study of air–sea interactions in the Gulf of Lion, where strong regional wind events can trigger marine convection (Lebeaupin-Brossier and Drobinski 2009; Lebeaupin-Brossier et al. 2011). These winds are called mistral and tramontana. Tramontana blows from the northwest and is channeled by the Pyrenees and the Massif Central mountains. Without orographic forcing, tramontana diverges above the Mediterranean. The mistral is a northerly wind blowing over a thick layer in the Rhône valley, guided by the contours of the Massif Central and the Alps. The flow diverges over the

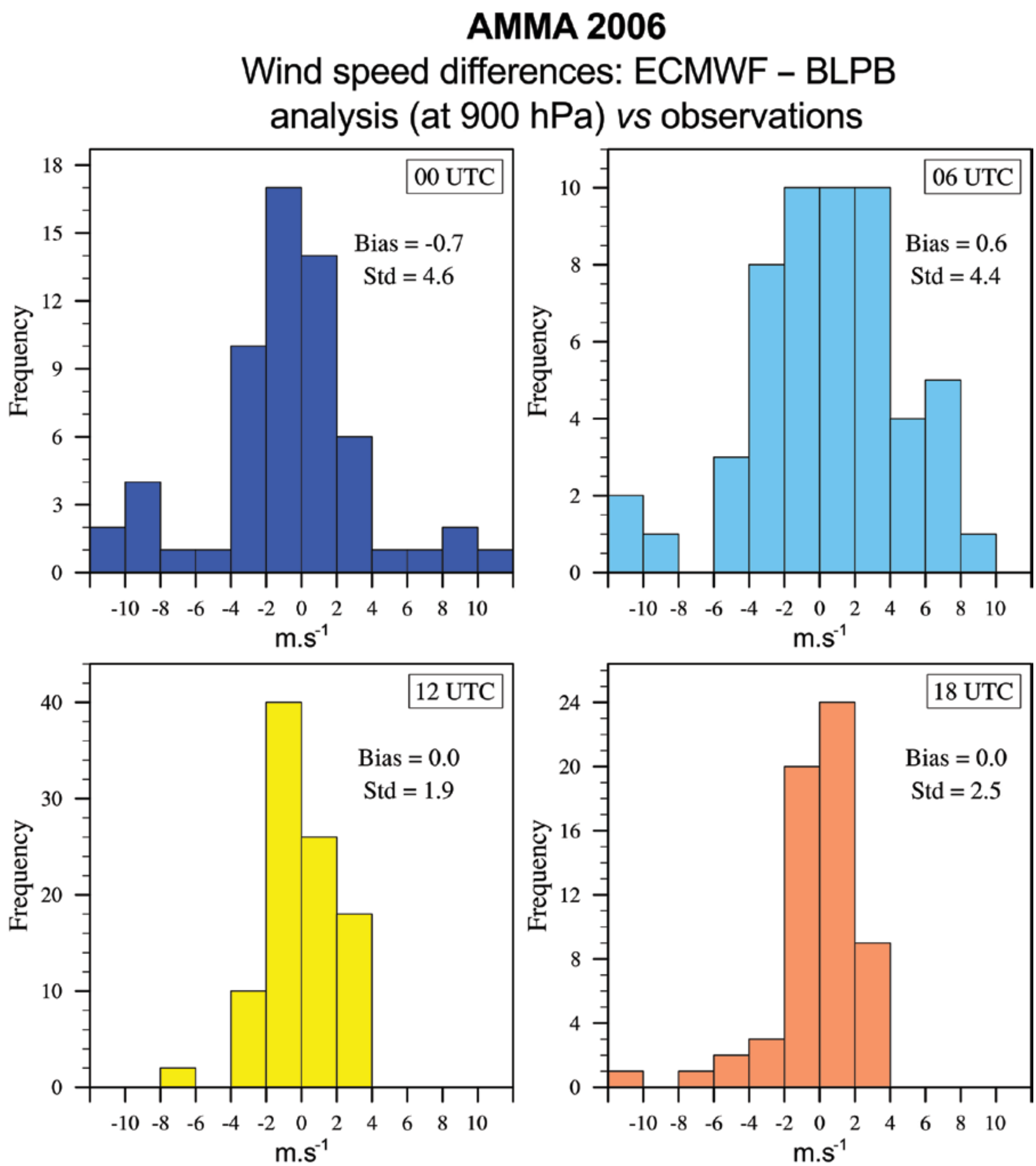

Fig. 9. Frequency histogram of the difference between the ECMWF wind speed at 925 hPa and the BLPB wind speed at (top left) 0000, (top right) 0600, (bottom left) 1200, and (bottom right) 1800 UTC. The bias and standard deviation, computed for all BLPBs, are indicated in each panel. See main text for comments.

Mediterranean Sea. During winter, the air parcels are generally dry and cold when they leave land and collect heat and humidity traveling over the warm Mediterranean Sea, as far as a few hundred kilometers from the coast. The air–sea interactions between the mistral and the waters off the coast of France drive in part the circulation of the Mediterranean Sea.

The 15 BLPBs were launched by the CNES with the aim of documenting the evolution of these air masses as they traveled above the Mediterranean. These flights were also an opportunity to document the dynamics of these winds when they blow offshore in poorly monitored areas (Fig. 10, left).

The launch site was in Candillargues, in the coastal region close to Montpellier (France), where both the tramontana and mistral generally remain moderate. Low-wind environments support manual-launch procedures since balloons may be damaged when they hit the ground in turbulent winds. With a target flight level of 800 or 900 m, buoyancy at launch is not sufficient to combat turbulence near the ground.

BLPB trajectories commenced at moderate speeds, typically increasing during the first 150–200 km. BLPBs went up and down along their trajectories, indicating that these were not constant-level flights (Fig. 10, right). The convergence of mistral and tramontana generated large mixing with plentiful vertical movements. Despite these repeated changes in the flight altitude, it was possible to show the increase of humidity during the flights (Fig. 10, left). Flight B42 was peculiar, with a long portion of its flight having very low humidity (Fig. 10). This was a case where there was low tramontana. The balloon was launched by chance in a volume of very dry air that stayed intact for several hours above the Mediterranean before the mixing succeeded in breaking the isolation of the air parcel.

Individual flight data and graphs can be found online (at www.lmd.polytechnique.fr/BAMED/BAMED_BP_Flight_SOP2.php).

In HyMeX SOP2, dynamical processes driving the circulation of the mistral and tramontana, and particularly the wake formation downstream of the Massif Central, were investigated using the BLPBs. Little is known about the finescale structure, especially over the Mediterranean Sea, where highly resolved observations in time and space are lacking. Despite the waves not being isopycnic, the absence of flow recirculation (or wave breaking; see Schär and

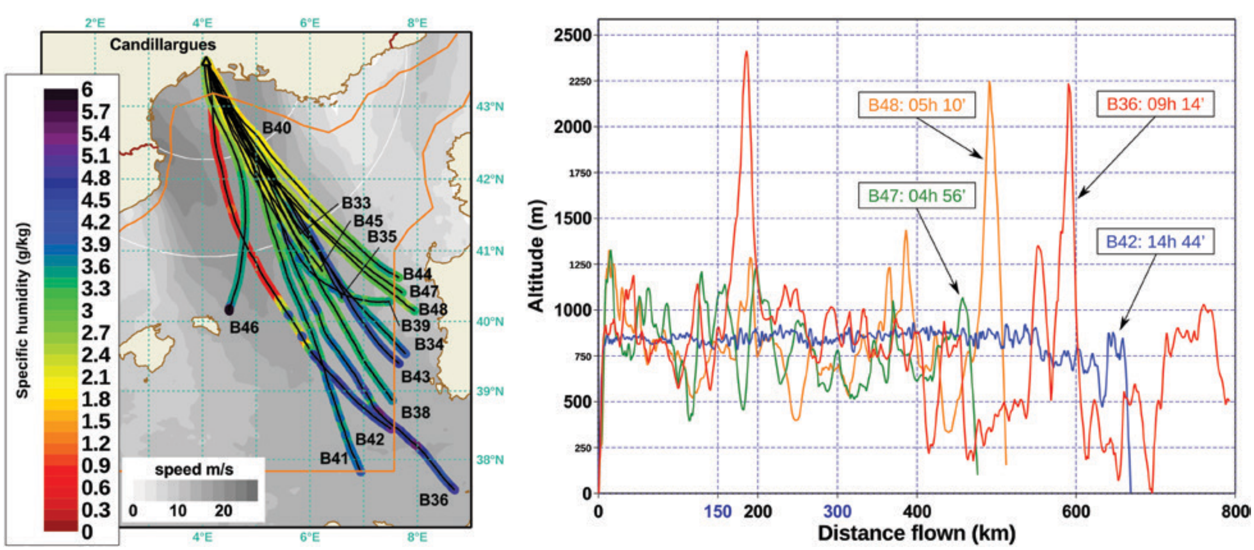

Fig. 10. (left) Trajectories of BLPBs during HyMeX SOP2 (15 flights). The color of the trajectories indicates the specific humidity measured during the flights. As in Fig. 6, the orange line depicts the limits of the flight domain. The flight segments outside this polygon correspond to the descending phase of the flight, which can be long if the flight level is high and in the case of strong winds. The gray shading shows mean wind speed from a weather model. The two white arcs show 150- and 300-km distances from Candillargues. (right) Flight altitude as a function of the distance flown for a selection of four HyMeX SOP2 flights. Flight duration is shown in the arrow boxes. The flight level is very chaotic for all except B42 (and B36 not shown), which corresponds to a moderate wind event. The cruise level is reached after 20 km or less. B47 and B48 have been launched simultaneously (see Fig. 1) but experienced different vertical excursions very early into their flights. Most SOP2 flights exhibited a series of ascents and descents, as a consequence of the very high level of turbulence induced by the convergence of the two regional winds; however, it can be seen that the humidity increases along the flights.

Smith 1993) and the moderate amplitude of the wakes allowed the BLPBS to collect a unique dataset in order to analyze in depth the finescale offshore dynamics of the mistral and tramontana (wake, convergence area, gravity waves, and convection). Figure 11 displays the wind speed of each balloon normalized by a constant value U_∞ that represents the speed of the undisturbed flow. The value of U_∞ was derived from the mean speed of each balloon at a great distance downstream of the shore (at the 150–300-km interval that can also be seen in Fig. 10). The average peak speed of the SOP2 balloons was, roughly, 30 m s^{-1}. All data closely cluster around a "single" curve. It shows clearly the reduced wind speed on the left of Fig. 11, with respect to U_∞, associated with the mountain wake, over a horizontal range of about 200 km from the coast. The wake is due to turbulent processes within the PBL and to gravity wave breaking (Drobinski et al. 2013).

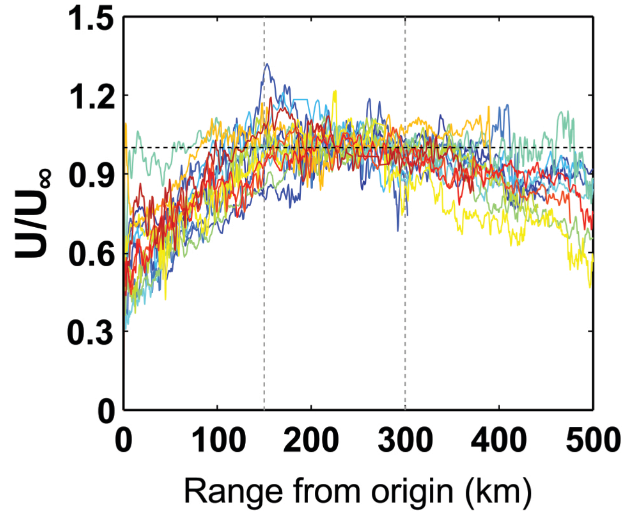

Fig. 11. BLPB wind speed normalized by the undisturbed flow speed U_∞ measured at a great distance downstream (150–300-km interval; see Fig. 10) of the balloon trajectories as a function of the distance to the launching site near the coast. The different curves correspond to the different BLPBs launched during HyMeX SOP2.

A novel application: Balloons as adaptive observation. The main objective of HyMeX SOP1 was to improve the knowledge and prediction capabilities of intense (even extreme) HPEs on the mountains surrounding the northwestern Mediterranean basin (Ducrocq et al. 2014). Nuissier et al. (2008) and Duffourg and Ducrocq (2011) show that the intensity and location of the HPEs depend on an appropriate description of the upstream humidity convergence above the sea. High density of wind and humidity observations in lower levels above the sea are therefore of great interest for an accurate prediction of HPEs. BLPBs appeared to be an appropriate observing platform with which to collect observations in this domain.

Furthermore, the HyMeX field phases included some adaptive (or targeted) observation aspects (Majumdar et al. 2014), especially during the first SOP. Data assimilation of targeted observations in NWP systems is expected to improve short-range forecasts. The improvement is defined as the difference between the forecast issued after additional observations have been assimilated and the forecast that would not have benefited from additional observations. Adaptive observation is very particular in the sense that the location and time of the additional observation are anticipated and chosen in order to reap the maximal benefit with the smallest observational change. During HyMeX SOP1, many observing systems collected data, but only some of these could provide NWP models with real-time upstream data for an adaptive observation usage.

The most obvious aspect of these targeting procedures was the implementation of the joint ECMWF–EUMETNET DTS procedure (Prates et al. 2009; Jansa et al. 2011), which allowed data from additional RS to be collected on demand from the HyMeX Operation Center. The chief forecasters at the HOC requested daily the extra RSs for the next day. The RS selection was made through the DTS web interface with the help of model sensitivity information, updated daily (Campins and Navascuès 2016).

The deployment of BLPBs as means of adaptive observation was not included in the integrated procedures of the DTS, but the HyMeX Operation Center requested the launch of BLPBs when appropriate. The main difficulty stemmed from the balloon's nature to drift that limited our ability to place the observing platform at the right location and at the right time. With a single launch site, the only degrees of freedom in terms of the control of the balloon's trajectories concerned the date and time of the launch and the flight level. To anticipate launches and to guarantee that the best launch time window was not missed (i.e., the starting point of the trajectory ending in the as-yet nonexisting but so far only predicted HPEs), a comprehensive set of isopycnic trajectories was predicted twice a day. The prediction of every possible trajectory allowed the HOC to avoid the use of sensitivity information when deciding on the launch of BLPBs.

Example of dataset in AROME-WMED data assimilation. High-frequency data (2 data packets per minute) from the BLPBs during HyMeX SOP1 and SOP2 were filtered to produce NWP-compatible data (1 data packet every 15 minutes) that were assimilated by the French operational NWP models ARPEGE (Courtier et al. 1991), AROME-France (Seity et al. 2011), and AROME-WMED (Fourrié et al. 2015). This was a novelty, as low-level drifting balloon data had never been assimilated into AROME before HyMeX. The procedure, called the BAMOBS, produced 828 reports during SOP1, about 700 of which entered the data assimilation procedures. During SOP2, 868 reports were issued. The HyMeX balloons' dataset is available through the HyMeX database (http://mistrals.sedoo.fr/HyMeX/).

The assimilated dataset is unprecedented, as very few in situ data exist at low levels above the sea. Figure 12 shows the horizontal and vertical density of BLPB observations versus all the other nonsatellite (in situ and radar) data in the BLPB domain. On the map (Fig. 12, left), the red square shows the area from which the observations have been extracted from the AROME observational database, and the orange line shows the BLPBs' flight domain. This domain is used to compute the vertical distribution (Fig. 12, right) of these data as a function of longitude and pressure, where the BLPBs data are shown in gray hatching. It is easy to see that BLPBs are complementary with other upper-air in situ observations, including reports from commercial aircraft and radiosoundings. Most of the radar radial wind data are out of the flight domain, and most aircraft data are in the vicinity of the airports of Barcelona (Spain), Marseille (France), and Nice (France) and therefore too close to the shore. The only lower-level aircraft data in the balloons' flight domain are close to the Balearic airports of Ibiza and Majorca. Most of the HyMeX radiosoundings at sea were made by the vessel *Le Provence* that remained close to the Gulf of Lion moored buoy and only during short periods of the SOP1. These repeated soundings produce the vertical gray stripe at 4.5°E longitude in Fig. 12 (right panel) and overlap the BLPBs dataset. The balloons, however, never flew in the vicinity of these soundings. Figure 12 shows that BLPBs have been able to collect data at low level, in the middle of the northwestern Mediterranean basin, a crucial region for the prediction of heavy-precipitation events (Duffourg and Ducrocq 2011) and where very few other observations were available for data assimilation and NWP.

CONCLUSIONS. CNES is experienced at operating low-level drifting balloons, as it has been doing so for more than three decades. Most campaigns took place overseas, INDOEX, VASCO-Cirene, and then HyMeX and ChArMEx, but also above land, as with AMMA. The years 2012 and 2013 with HyMeX and ChArMEx were highlighted for balloon activity in the Mediterranean. There were 66 constant-volume balloons deployed in 14 months in a variety of weather conditions and various scientific missions. These missions ranged from Lagrangian studies, for example, chemistry (ozone) and radiation (aerosols), to process studies such as humidity uptake above the Mediterranean and observation for real-time data assimilation.

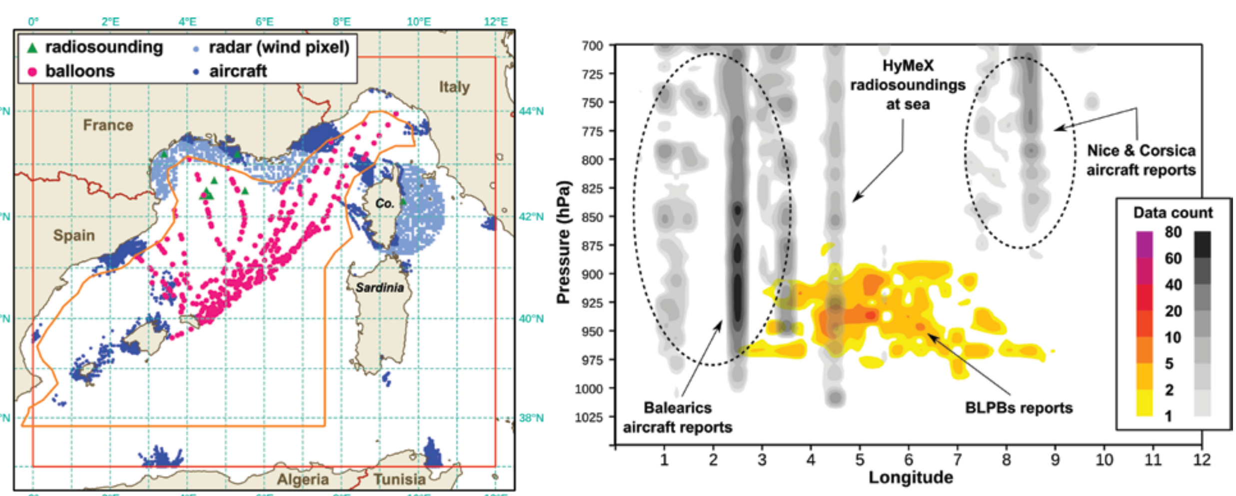

Fig. 12. Distribution of nonsatellite observations above the sea exploited in the AROME-WMED data assimilation procedure during the entire SOP1 of HyMeX (2 months). (left) Each point on the map is an assimilated observation (temperature or wind) below 700 hPa. The area outlined in orange is the BLPB flight domain. (right) The vertical longitude–pressure cross section shows data counts in 0.1° × 0.1° × 10 hPa boxes that have been averaged in latitude in the red square domain on the map. These two views show that BLPBs (yellow-orange colors) provide observations where no other nonsatellite system (gray scale) can provide observations.

BLPBs are almost ideal observational platforms for Lagrangian studies of chemicals and dust transport, especially as the scientific approach requires calm and dry weather conditions. It is worth emphasizing the balloons' ability to last for several weeks when their flight domain is sufficiently wide enough and when optimized power consumption allows for such a duration.

BLPBs also proved able to cope with a variety of weather conditions and nonquiet weather situations, sometimes leading to an anticipated end of flight. During AMMA, BLPBs faced African monsoon weather, including convection and low-level jet. In HyMeX SOP2, BLPBs met strong (up to 115 km h^{-1}) and turbulent winds and underwent frequent vertical excursions, which often exceeded 500 m, but without any balloon losses. In HyMeX SOP1, the early end of flight for four BLPBs is attributed to weather such as precipitation (one case) and strong convective activity (three cases). This represents a small portion of the flights, knowing that some BLPBs traveled at about 90 km h^{-1} at only 300 m above the sea. With this taken into consideration, BLPB is thought to be a reliable platform, bearing in mind that it is simply a drifting balloon!

Despite the fact that all the aforementioned flight conditions are depreciative for strict Lagrangian studies, BLPBs succeeded in collecting valuable datasets. In AMMA, BLPBs succeeded in investigating the diurnal cycle in the Sahel. Flights in HyMeX-SOP2 allowed the study of the wind structure and sampling of the marine humidity uptake. Finally, considering adaptive observation for data assimilation, HyMeX SOP1 flights allowed the collecting of valuable observations in active weather areas.

From experience during recent campaigns, a few improvements in the design of the BLPBs would be welcomed. These include access to renewable energy sources, in-flight control of the buoyancy (even limited), fully recoverable sea landing, and enhanced observing capabilities. For example, measurement of in situ precipitation along flights over sea is nearly at hand with BLPBs; this would be of incomparable value.

ACKNOWLEDGMENTS. The authors would like to acknowledge the importance of the MISTRALS/ChArMEx and MISTRALS/HyMeX programs as well as the support of LEFE and TOSCA and the funding by ANR under Contract IODA-MED ANR-11-BS56-0005. The BLPB field campaigns in the Mediterranean would not have been possible without the motivation of local people who hosted the launch sites during HyMeX and ChArMEx as well as the willingness of air traffic control agents.

The scientific community collected unique datasets during these campaigns, thanks to the CNES, its balloons department, and the very professional and motivated staff.

A special thank you is extended to Jean-Noël Valdivia for his support concerning technology in the gondolas and to Naomi Riviere and Alan Hally for their support concerning the language.

Finally the coauthors would like to thank Météo-France, LMD, Alain Fontaine, and the SEDOO group for the meteorological data and tools that allowed the setting up of the trajectory prediction facility in both HyMeX and ChArMEx.

APPENDIX: LIST OF ACRONYMS.

3D	Three-dimensional
ADRIMED	Aerosol Direct Radiative Impact on the Regional Climate in the Mediterranean
AMMA	African Monsoon Multiscale Analysis
AROME	Applications of Research to Operations at Mesoscale
ARPEGE	Action de Recherche Petite Echelle Grande Echelle
ASL	Above sea level
BAMED	Balloons in the Mediterranean
BAMOBS	BAMED Observation System
BLPB	Boundary layer pressurized balloon
ChArMEx	Chemistry–Aerosol Mediterranean Experiment
CNES	Centre National d'Études Spatiales (French Space Agency)
DTS	Data Targeting System
ECC	Electrochemical concentration cell (ozonesonde)
ECMWF	European Centre for Medium-Range Weather Forecasts
EQR	Equator
EUMETNET	European National Meteorological Services
GNSS	Global Navigation Satellite System
GPS	Global positioning system

HOC	HyMeX Operation Centre
HPE	Heavy-precipitation event
HyMeX	Hydrological Cycle in the Mediterranean Experiment
ICAO	International Civil Aviation Organization
INDOEX	Indian Ocean Experiment
IO	Indian Ocean
ITCZ	Intertropical convergence zone
ITD	Intertropical discontinuity
LOAC	Light optical aerosols counter
LPC2E	Laboratoire de Physique et Chimie de l'Environnement et de l'Espace
Meteosat	Meteorological Satellite
MJO	Madden–Julian oscillation
MSL	Above mean sea level
NOAA	National Oceanic and Atmospheric Administration
NPH	North Pole Housekeeping (gondola)
NPS	North Pole Scientific (gondola)
NWMed	Northwestern Mediterranean
NWP	Numerical Weather Prediction
PBL	Planetary boundary layer
RS	Radiosounding
SAFIRE	Service des Avions Francais Instrumentes pour la Recherche en Environnement
SAF-MED	Secondary Aerosol Formation in the Mediterranean
SOP	Special Observing Period
SPH	South Pole Housekeeping (gondola)
SPS	South Pole Scientific (gondola)
TRAQA	Transport à Longue Distance et Qualité de l'Air dans le bassin Méditerranéen (Long Distance Transport and Air Quality in the Mediterranean basin)
UHF	Ultrahigh-frequency
VASCO	Validation of the Aeroclipper System under Convective Occurrence
WA	Western Africa
WMED	Western Mediterranean

REFERENCES

Bénech, B., A. Druilhet, R. Cordesse, B. Dartigues-Longues, J. Fournet-Fayard, J.-C. Mesnager, P. Durand, and A. Malaterre, 1987: Un dispositif expérimental utilisant des ballons plafonnants pour l'étude de la couche limite atmosphérique. *Adv. Space Res.*, **7** (7), 77–83, doi:10.1016/0273-1177(87)90012-3.

——, A. Ezcurra, M. Lothon, F. Saïd, B. Campistron, F. Lohou, and P. Durand, 2008: Constant volume balloons measurements in the urban Marseille and Fos–Berre industrial ozone plumes during ESCOMPTE experiment. *Atmos. Environ.*, **42**, 5589–5601, doi:10.1016/j.atmosenv.2008.03.011.

Businger, S., S. Chiswell, W. Ulmer, and R. Johnson, 1996: Balloons as a Lagrangian measurement platform for atmospheric research. *J. Geophys. Res.*, **101**, 4363–4376, doi:10.1029/95JD00559.

——, R. Johnson, and R. Talbot, 2006: Scientific insights from four generations of Lagrangian smart balloons in atmospheric research. *Bull. Amer. Meteor. Soc.*, **87**, 1539–1554, doi:10.1175/BAMS-87-11-1539.

Cadet, D., H. Ovarlez, and G. Sommeria, 1981: The BALSAMINE experiment during the summer MONEX. *Bull. Amer. Meteor. Soc.*, **62**, 381–388.

Campins, J., and B. Navascuès, 2016: Impact of targeted observations on HIRLAM forecasts during HyMeX-SOP1. *Quart. J. Roy. Meteor. Soc.*, doi:10.1002/qj.2737, in press.

Courtier, P., C. Freydier, J. F. Geleyn, F. Rabier, and M. Rochas, 1991: The ARPEGE project at Météo-France. *ECMWF Seminar Proc.*, Shinfield Park, Reading, United Kingdom, ECMWF, 193–231.

Drobinski, P., C. Basdevant, A. Doerenbecher, P. Cocquerez, F. Bernard, S. Berthou, P. Jourdier, and A. Di Luca, 2013: Preliminary analysis of tramontane/mistral offshore dynamics during HyMeX SOP2 from the boundary layer pressurized balloons. *Proc. Seventh HyMeX Workshop*, Cassis, France, CNRS, PS2.14.

Drobinski, P., and Coauthors, 2014: HyMeX, a 10-year multidisciplinary program on the Mediterranean water cycle. *Bull. Amer. Meteor. Soc.*, **95**, 1063–1082, doi:10.1175/BAMS-D-12-00242.1.

Ducrocq, V., and Coauthors, 2014: HyMeX-SOP1: The field campaign dedicated to heavy precipitation and flash-flooding in the northwestern Mediterranean. *Bull. Amer. Meteor. Soc.*, **95**, 1083–1100, doi:10.1175/BAMS-D-12-00244.1.

Duffourg, F., and V. Ducrocq, 2011: Origin of the moisture feeding the heavy precipitating systems over southeastern France. *Nat. Hazards Earth Syst. Sci.*, **11**, 1163–1178, doi:10.5194/nhess-11-1163-2011.

Duvel, J.-P., C. Basdevant, H. Bellenger, G. Reverdin, A. Vargas, and J. Vialard, 2009: The Aeroclipper: A new device to explore convective systems and cyclones. *Bull. Amer. Meteor. Soc.*, **90**, 63–71, doi:10.1175/2008BAMS2500.1.

Ethé, C., C. Basdevant, R. Sadourny, K. S. Appu, L. Harenduprakash, P. R. Sarode, and G. Viswanathan, 2002: Air mass motion, temperature, and humidity over the Arabian Sea and western Indian Ocean during the INDOEX intensive phase, as obtained from a set of superpressure drifting balloons. *J. Geophys. Res.*, **107**, 8023, doi:10.1029/2001JD001120.

Fourrié, N., and Coauthors, 2015: AROME-WMED, a real-time mesoscale model designed for the HyMeX special observation periods. *Geosci. Model Dev.*, **8**, 1919–1941, doi:10.5194/gmd-8-1919-2015.

ICAO, 2005: Appendix 4. Rules of the Air, International Civil Aviation Organization, APP 4-1–APP 4-4. [Available online at www.horoug.com/horoug_files/icao_regulations/ICAO%20Annex%202%20-%20Rules%20of%20the%20Air.pdf.]

Jansa, A., and Coauthors, 2011: A new approach to sensitivity climatologies: The DTS-MEDEX-2009 campaign. *Nat. Hazards Earth Syst. Sci.*, **11**, 2381–2390, doi:10.5194/nhess-11-2381-2011.

Lebeaupin Brossier, C., and P. Drobinski, 2009: Numerical high-resolution air-sea coupling over the Gulf of Lions during two tramontane/mistral events. *J. Geophys. Res.*, **114**, D10110, doi:10.1029/2008JD011601.

——, K. Béranger, C. Deltel, and P. Drobinski, 2011: The Mediterranean response to different space-time resolution atmospheric forcings using perpetual mode sensitivity simulations. *Ocean Modell.*, **36**, 1–25, doi:10.1016/j.ocemod.2010.10.008.

Lebel, T., and Coauthors, 2010: The AMMA field campaigns: Multiscale and multidisciplinary observations in the West African region. *Quart. J. Roy. Meteor. Soc.*, **136**, 8–33, doi:10.1002/qj.486.

Lelieveld, J., and Coauthors, 2001: The Indian Ocean experiment: Widespread air pollution from South and Southeast Asia. *Science*, **291**, 1031–1036, doi:10.1126/science.1057103.

Majumdar, S. J., and Coauthors, 2014: Targeted observation for improving numerical weather prediction: An overview. WMO WWRP/THORPEX Rep. 15, 37 pp.

Nuissier, O., V. Ducrocq, D. Ricard, C. Lebeaupin, and S. Anquetin, 2008: A numerical study of three catastrophic precipitating events over southern France. I: Numerical framework and synoptic ingredients. *Quart. J. Roy. Meteor. Soc.*, **134**, 111–130, doi:10.1002/qj.200.

Prates, C., D. Richardson, and C. Sahin, 2009: Final report of the PREVIEW observation Data Targeting System (DTS). ECMWF Tech. Memo. 581, 31 pp. [Available online at www.ecmwf.int/sites/default/files/elibrary/2009/11720-final-report-preview-observation-data-targeting-system-dts.pdf.]

Redelsperger, J.-L., C. Thorncroft, A. Diedhiou, T. Lebel, D. J. Parker, and J. Polcher, 2006: African Monsoon Multidisciplinary Analysis: An international research project and field campaign. *Bull. Amer. Meteor. Soc.*, **87**, 1739–1746, doi:10.1175/BAMS-87-12-1739.

Renard, J.-B., and Coauthors, 2015: LOAC: A small aerosol optical counter/sizer for ground-based and balloon measurements of the size distribution and nature of atmospheric particles—Part 2: First results from balloon and unmanned aerial vehicle flights. *Atmos. Meas. Tech.*, **8**, 10 057–10 096, doi:10.5194/amtd-8-10057-2015, in press.

——, and Coauthors, 2016: LOAC: A small aerosol optical counter/sizer for ground-based and balloon measurements of the size distribution and nature of atmospheric particles—Part 1: Principle of measurements and instrument evaluation. *Atmos. Meas. Tech.*, **9**, 1721–1742, doi:10.5194/amt-9-1721-2016.

Schär, C., and R. B. Smith, 1993: Shallow water flow past isolated topography. Part I: Vorticity production and wake formation. *J. Atmos. Sci.*, **50**, 1373–1400, doi:10.1175/1520-0469(1993)050<1373:SWFPIT>2.0.CO;2.

Seity, Y., P. Brousseau, S. Malardel, G. Hello, P. Bénard, F. Bouttier, C. Lac, and V. Masson, 2011: The AROME-France convective-scale operational model. *Mon. Wea. Rev.*, **139**, 976–991, doi:10.1175/2010MWR3425.1.

Sultan, B., S. Janicot, and P. Drobinski, 2007: Characterization of the diurnal cycle of the West African monsoon around the monsoon onset. *J. Climate*, **20**, 4014–4032, doi:10.1175/JCLI4218.1.

Vialard, J., and Coauthors, 2009: CIRENE: Air–sea interactions in the Seychelles–Chagos thermocline ridge region. *Bull. Amer. Meteor. Soc.*, **90**, 45–61, doi:10.1175/2008BAMS2499.1.